

# Magnetic resonance imaging anatomy of the craniovertebral ligaments: A radiological study with confirmatory dissection

## ABSTRACT

**Background:** Descriptions of the radiological appearance of the craniovertebral ligaments often lack detail. This study aimed to provide an accurate description of the morphology and radiological appearance of the alar and cruciform ligaments with confirmation of findings by fine dissection.

**Materials and Methods:** Six embalmed human cadaveric specimens were reduced to an osseoligamentous arrangement spanning the C2/3 disc to the occiput. Specimens were imaged on a 4.6T Bruker magnetic resonance (MR) system using a 3D RARE multiple SE sequence with acquisition time 18 h 24 min. Acquired images were viewed in three planes, and detailed descriptions and morphometric measurement of the ligaments were obtained. Specimens were then examined and described using fine dissection. Direct comparison of the descriptions of each method was undertaken.

**Results:** From imaging, detailed features of all alar ligaments could be identified in all specimens. Consistency in shape, orientation, and attachments is described. Attachment to the medial aspect of the atlantooccipital joints was evident in all specimens. Five of six alar ligament pairs contained fibers that traversed the dens without attachment. Ascending cruciform ligaments could be clearly identified in four of six specimens. No descending cruciform ligaments could be clearly delineated. Detailed features of the transverse ligaments could be identified and described in all planes. Dissection findings were mostly consistent with descriptions obtained from MR images.

**Conclusion:** 4.6T MR images provide accurate detail of the structure, dimensions, and attachments of the craniovertebral ligaments. The morphology of the craniovertebral ligaments assessed radiologically was consistent with findings on gross dissection.

**Keywords:** Craniocervical anatomy, craniovertebral, ligament, magnetic resonance imaging

## INTRODUCTION

Injury to the ligaments of the craniovertebral region, whether due to trauma or disease, has the potential to predispose the region to altered kinematics and clinical instability.<sup>[1-5]</sup> The diagnosis of irregularities of the craniovertebral ligaments by medical imaging is predicated by a presumed understanding of the normal radiological appearance of these ligaments. Descriptions of the radiological appearance of these ligaments often lack detail and are, at times, contradictory. As a consequence, the radiological clinical assessment of pathological changes in these structures may be lacking in certainty because there is not a systematic description of the morphology from which to work.

Magnetic resonance imaging (MRI) is currently accepted as the most accurate method of depicting the craniocervical

**PETER GRANT OSMOTHERLY,  
GARY J. COWIN<sup>1</sup>, DARREN A. RIVETT**


School of Health Sciences, The University of Newcastle, Callaghan, <sup>1</sup>Centre For Advanced Imaging, The University of Queensland, Brisbane, Australia

**Address for correspondence:** Dr. Peter Grant Osmotherly, School of Health Sciences, The University of Newcastle, Callaghan NSW 2308, Australia.  
E-mail: peter.osmotherly@newcastle.edu.au

**Submitted:** 27-Apr-22

**Accepted:** 08-May-22

**Published:** 14-Sep-22

| Access this article online               |   |
|--|---|
| <b>Website:</b><br>www.jcvjs.com         | <b>Quick Response Code</b><br> |
| <b>DOI:</b><br>10.4103/jcvjs.jcvjs_62_22 |   |

This is an open access journal, and articles are distributed under the terms of the Creative Commons Attribution-NonCommercial-ShareAlike 4.0 License, which allows others to remix, tweak, and build upon the work non-commercially, as long as appropriate credit is given and the new creations are licensed under the identical terms.

**For reprints contact:** WKHLRPMedknow\_reprints@wolterskluwer.com

**How to cite this article:** Osmotherly PG, Cowin GJ, Rivett DA. Magnetic resonance imaging anatomy of the craniovertebral ligaments: A radiological study with confirmatory dissection. J Craniovert Jun Spine 2022;13:309-17.

ligaments, particularly the alar and transverse ligaments.<sup>[6]</sup> In all clinical MRI, a contrast between areas of high signal intensity and areas of low-signal intensity must be present to demonstrate both normal anatomical features and abnormalities.<sup>[7]</sup> Despite improvements in imaging techniques, identification and delineation of all aspects of the alar and cruciform ligaments in all planes remain difficult. The alar ligaments have been described as showing a low-to-intermediate signal intensity,<sup>[8]</sup> often with low-signal laterally and a higher signal medially.<sup>[9]</sup> However, identification and description of the alar ligaments in normal study populations have often been incomplete, particularly in the sagittal plane where epidural fat surrounding the ligaments makes differentiation of the ligaments and interpretation of the resultant images difficult as the fat surrounding the alar ligaments has a similar signal intensity to the ligaments themselves.<sup>[10,11]</sup>

A similar situation is evident in the examination of the transverse ligament. While the transverse ligament is discernible in nearly all cases using MRI<sup>[12,13]</sup> with the ligament appearing as a relatively homogeneous low-signal intensity structure, differentiation of the margins of the ligament is often less clear due to the presence of other low-signal intensity soft tissues surrounding the odontoid process including epidural fat, the tectorial membrane and the dura mater<sup>[9,12]</sup> making accurate delineation and description of the transverse ligament difficult.

The current study aims to provide greater detail regarding the radiological appearance of the alar and cruciform ligaments. By examining these structures under high-definition MRI, a more accurate description of their morphology and radiological appearance may be achieved. Confirmation of radiological observations by fine dissection provides an added measure of validity to the findings evinced by the high-resolution imaging of these ligamentous structures.

## MATERIALS AND METHODS

Six cervical spine and head specimens were obtained from embalmed human cadavers (2 females, 4 males, mean age 81.2 years standard deviation 12.6 years, range 58 to 94 years). No cadaveric material had a listed cause of death due to trauma. All cadaveric material was supplied by the Department of Anatomy and Developmental Biology, School of Biomedical Sciences, The University of Queensland. All cadavers used in this study were donated in accordance with the Queensland Transplantation and Anatomy Act 1979 (as amended). Ethical approval for this study was obtained from the University of Queensland.

Specimens were reduced to a section spanning the interval of the occiput to the level of the C2/3 intervertebral disc. Specimens were then divested of all muscle tissue, leaving an osteoligamentous arrangement of a size which could be encased in the bore of the 4.6T MRI scanner. Each specimen was prepared using an approach based on the dissection technique described by Dvorak *et al.*<sup>[14]</sup> A posterior wedge of approximately 140° was removed from the occipital bone. The posterior arch of the atlas was then resected, and a wide laminectomy was performed to remove the posterior elements of the axis, thereby exposing the internal soft tissue elements of the vertebral canal.

Prior to imaging, each specimen was hydrated for 24 h in a 20% propylene glycol solution to enhance response to the MRI signal. Specimens were then encased in 65 mm diameter plastic cylinders. The space surrounding the specimens was filled with Fomblin oil, a high-density perfluoropolyether derivative, to minimize vibration movement of the specimen during scanning. The use of Fomblin also provides improved image contrast as it provides a completely dark background on the MR image since it does not contain hydrogen protons.<sup>[15]</sup>

High-resolution images were acquired on a Bruker (Ettlingen, Germany) animal MRI system consisting of a 4.6T magnet interfaced to an AVANCE spectrometer running ParaVision 4.0. A 3D RARE multiple spin echo sequence was used with the following parameters: TR = 2 sec, echo train length = 8, effective TE = 56, SW = 100000Hz, field-of-view (FOV) = 80 mm × 80 mm × 45 mm, acquisition matrix = 512 × 512 × 256, and image resolution = 0.156 mm × 0.156 mm × 0.176 mm. The total acquisition time for each specimen was 18 h, 24 min.

Data were collected from all acquired images with viewing in three orthogonal planes; sagittal, coronal, and axial. Detailed descriptions of the structure and the attachment sites of each ligament were recorded. Morphometric measurements were made for each ligament. For the alar ligaments, measures included length, cephalocaudal height, anteroposterior width, attachment distance in relation to the tip of the odontoid process, and angle of orientation of the ligaments in both coronal and axial planes. Transverse ligament measures included cephalocaudal height, anteroposterior thickness, and length of both anterior and posterior margins of the ligament in axial section.

Following imaging, each specimen was dissected in a manner consistent with the methods previously given in descriptive anatomical studies.<sup>[16]</sup> The ascending and descending

cruciform ligaments, the transverse ligament of the atlas and the alar ligaments were examined by fine dissection. Each structure was systematically dissected by resection of collagen bundles small enough to be grasped with sharpened jeweler's forceps. As bundles were stripped and removed, the orientation, location, and attachment sites were recorded descriptively and photographically. Superficial layers were resected to reveal deep layers which were then resected in a similar manner.

Descriptions derived from dissection of each specimen were then compared to the descriptions derived from examination of each specimen at high resolution. Direct comparison of these findings was used to confirm that the high-resolution images were reflective of the actual anatomical structure of the specimens.

## RESULTS

### Analysis of the 4.6T imaging of the alar and transverse ligaments.

#### Alar ligaments

The structure, borders and attachments of the alar ligaments could be reliably viewed in all six specimens passing from odontoid process to occiput. Each alar ligament consisted of fibers running longitudinally between two definable regions of bony attachment.

On a coronal view, each alar ligament could be seen to be substantially originating from the lateral and posterolateral aspect of the superior portion of the odontoid process. The length of attachment down the odontoid process was substantial, often encompassing the majority of its length. The origin was always below the tip of the odontoid process, attaching on average 1.8 mm inferior to it [Figure 1].

The alar ligaments passed laterally toward their attachments onto the occipital condyles. The average length of the ligaments was 9.5 mm (range 6.9–11.1 mm). On their path laterally, the ligaments reduced in measured superior-inferior height, producing a tapered appearance from an average height medially of 7 mm down to 3.5 mm laterally.

Insertion could be clearly visualized occurring into the medial aspect of the inferior portion of the occipital condyles, slightly superior and anterior to the atlantooccipital joints. In all six specimens, inferior fibers of the alar ligaments could also be seen to blend with the medial aspect of the atlantooccipital joints providing the appearance of a distinct contribution of the alar ligaments to the medial aspect of the joint itself [Figure 2].



**Figure 1:** The alar ligaments in coronal section acquired using imaging at 4.6T. The fibres of the ligament can be seen passing in a lateral direction between the odontoid process and the occiput. Attachment to the odontoid process is below the level of the tip as indicated by the arrow

The orientation of each alar ligament was measured with respect to the midline of the odontoid process. The method of calculating this angle is indicated in Figure 3. The orientation appeared to be primarily horizontal in five of the six specimens, with angles measured between 81° and 94°. One specimen was observed to have a distinctly shorter odontoid process relative to the occipital condyles. The alar ligaments in this specimen assumed a more cranial orientation measured as 114° and 111°. Side-to-side asymmetry was common with variation in the direction of ligament orientation observed within individual specimens. A detailed description of individual ligament characteristics in coronal view in each specimen is provided in Table 1.

On sagittal view, the alar ligaments were examined in cross-section along their course. Medially, the cross-sectional shape was primarily round with a mean diameter in these specimens of 5.1 mm. Viewed in cross-section toward their insertion, five ligaments had become more ovoid in shape due to a reduction in height. One had assumed a crescent shape with the convex surface facing posterosuperiorly. Mean dimensions of the alar ligaments in cross-section were 6.3 mm in the anteroposterior direction and 2.9 mm in the superior-inferior direction. The cross-sectional shape of the alar ligaments is indicated in Figure 4a and b.

In axial view, the alar ligaments could be very clearly delineated along their entire path from dens to the occiput [Figure 5]. The fibers of each alar ligament were oriented in a medial-lateral direction between these points of bony attachment. The length of each ligament was measured in this plane, averaging 10.2 mm, with a mean

**Table 1: Measurements and observations obtained from 4.6-tesla magnetic resonance imaging examination of the alar ligaments in coronal view**

| Specimen number | Length – medial to lateral (mm) | Height – medial (mm)      | Height – lateral (mm)     | Distance of attachment below tip of odontoid process (mm) | Orientation with respect to vertical axis of odontoid process (°) | Attachment into O-C1 medial joint capsule |
|-----------------|---------------------------------|---------------------------|---------------------------|---|---|---|
| 1               | Left - 11.1<br>Right - 11.1     | Left - 6.7<br>Right - 6.7 | Left - 3.2<br>Right - 3.8 | 0.0   | Left - 91.8<br>Right - 94.0                                       | Visible                                   |
| 2               | Left - 10.0<br>Right - 10.7     | Left - 7.4<br>Right - 8.7 | Left - 3.5<br>Right - 4.4 | 2.9   | Left - 88.3<br>Right - 91.7                                       | Visible                                   |
| 3               | Left - 8.2<br>Right - 9.0       | Left - 7.8<br>Right - 8.1 | Left - 2.6<br>Right - 4.5 | 2.7   | Left - 85.6<br>Right - 88.3                                       | Visible                                   |
| 4               | Left - 8.8<br>Right - 10.6      | Left - 5.3<br>Right - 4.6 | Left - 3.0<br>Right - 2.3 | 2.6   | Left - 87.2<br>Right - 81.0                                       | Visible                                   |
| 5               | Left - 7.7<br>Right - 6.9       | Left - 4.8<br>Right - 5.9 | Left - 3.7<br>Right - 4.1 | 0.7   | Left - 114.3<br>Right - 111.3                                     | Visible                                   |
| 6               | Left - 8.4<br>Right - 11.0      | Left - 9.4<br>Right - 8.7 | Left - 3.5<br>Right - 3.6 | 2.1   | Left - 87.4<br>Right - 89.8                                       | Visible                                   |

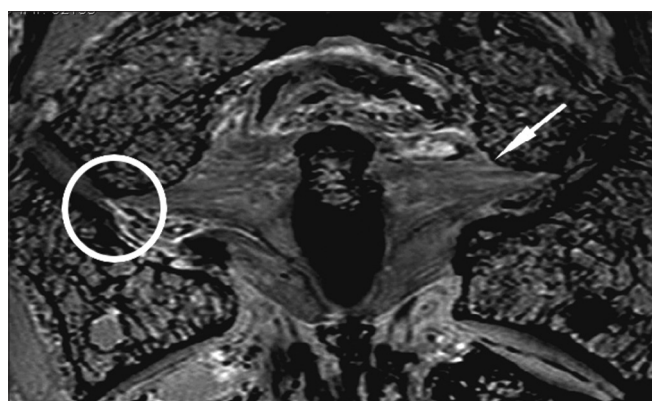


**Figure 2: Alar ligaments in coronal view acquired using imaging at 4.6T. Attachment onto the occiput is indicated by the arrow. Blending of the inferior fibres of the alar ligament into the medial aspect of the atlantooccipital joint is indicated by the circled area**

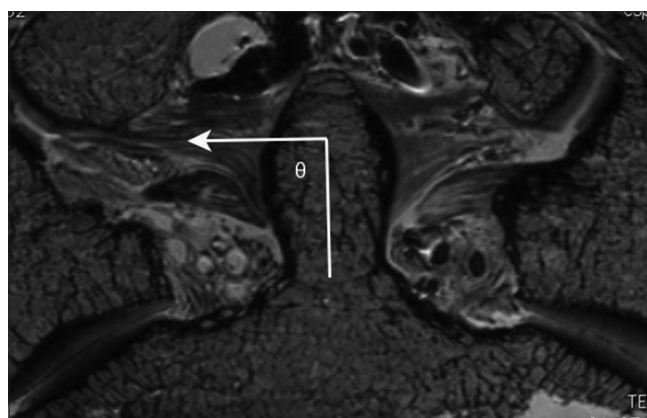


**Figure 3: Calculation of the angle of orientation of the alar ligaments with respect to the midline of the odontoid process. The measured angle is indicated by the symbol  $\theta$ . Image acquired at 4.6T**

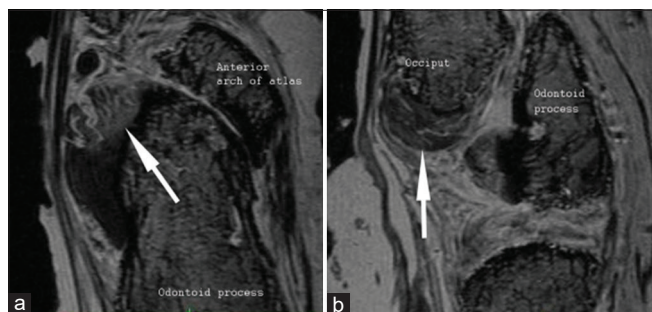


**Figure 4: Sagittal views demonstrating the alar ligaments in cross section (indicated by arrows) acquired using imaging at 4.6T. (a) Medial aspect, (b) Lateral aspect**

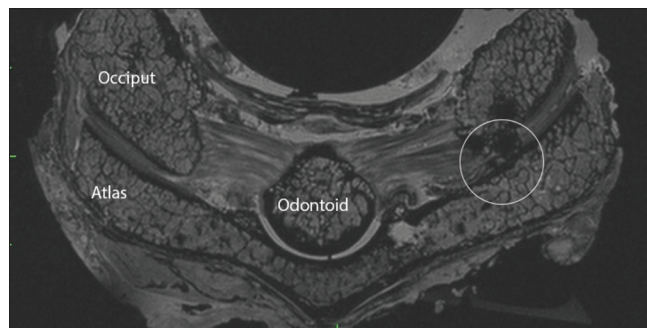


**Figure 5: The alar ligaments viewed in axial section acquired using imaging at 4.6T. Fibre orientation is visible medial to lateral between the odontoid process and the occipital condyle attachments. Fibres of the alar ligament blending into the medial aspect of the atlanto-occipital joint indicated by circled region**

width immediately distal to the odontoid process of 4.3 mm. The ligaments each passed in an obliquely posterior direction creating an average included angle between the ligaments of 137.4°. A detailed description of individual ligament characteristics in axial view in each specimen is provided in Table 2.

As noted in the coronal examination, an element of the anterior fibers of the alar ligaments could be traced back to a communication with the medial aspect of the atlantooccipital joint when viewed in horizontal section. However, unlike the coronal view, this could not be clearly visualized in all

specimens. Of the 12 alar ligaments examined, only six could be clearly seen to provide a contribution to the medial aspect of the atlantooccipital joint [Figure 5].

Five of the six pairs of alar ligaments also contained a proportion of fibers that completely traversed the dens without attachment [Figure 6]. The breadth of these bands varied between specimens with a mean thickness over six specimens of 1.0 mm. In the five specimens where this was evident this band comprised approximately 27% of the anteroposterior width of the ligament.

No portion of the alar ligament indicating an atlantal attachment was noted in any viewed plane in any specimen examined.

#### Ascending and descending cruciform ligaments

Ascending and descending cruciform ligaments were assessed using a sagittal section. This section was obtained by selecting a midline plane in the coronal section passing through the center of the odontoid process [Figure 7].

Ascending cruciform ligaments could be viewed in four of the six specimens examined. They consisted of an upward

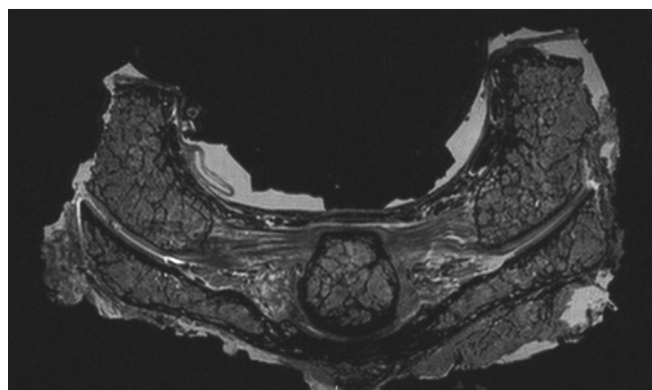


Figure 6: The alar ligaments viewed in axial section acquired using imaging at 4.6T. Fibres of the alar ligaments traversing the odontoid process

projection from the superior portion of the transverse ligament. The points of attachment of each ligament, as well as their anterior and posterior borders, were poorly defined in this view. Where present, ascending cruciform ligament length ranged from measured lengths of 7.6 mm to 14.7 mm, with an average length of 11.0 mm.

No descending cruciform ligaments could be clearly identified or meaningfully measured in any sequence examined.

#### Transverse ligament

The transverse ligament could be clearly defined on both axial and sagittal plane images. All endpoints and borders of this structure could be accurately marked for description and measurement purposes.

In midline sagittal view, the transverse ligament appears in cross-section as a dense elliptical structure located posteriorly against the dens [Figure 7]. Measured anteroposteriorly, the transverse ligaments examined had a mean thickness of

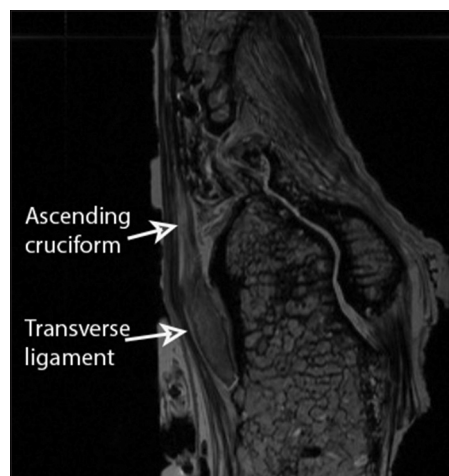


Figure 7: Ascending cruciform ligament and transverse ligament in sagittal view. Image acquired at 4.6T

Table 2: Measurements and observations obtained from 4.6-tesla magnetic resonance imaging examination of the alar ligaments in axial view

| Specimen number | Length (mm)                 | Width immediately distal to odontoid process (mm) | Included angle between alar ligaments | Attachment into O-C1 medial joint capsule | Depth of fibers traversing odontoid process (mm) |
|-----------------|-----------------------------|---|---------------------------------------|---|--|
| 1               | Left - 10.7<br>Right - 10.9 | Left - 3.6<br>Right - 3.4                         | Posterior<br>172.9°                   | Left visible<br>Right visible             | 0.3  |
| 2               | Left - 11.7<br>Right - 9.5  | Left - 4.8<br>Right - 4.1                         | Posterior<br>147.7°                   | Left visible<br>Right visible             | 0  |
| 3               | Left - 10.6<br>Right - 10.2 | Left - 4.3<br>Right - 4.2                         | Posterior<br>120.9°                   | Left not visible<br>Right not visible     | 0.8  |
| 4               | Left - 10.7<br>Right - 10.9 | Left - 4.9<br>Right - 5.3                         | Posterior<br>119.4°                   | Left not visible<br>Right not visible     | 2.2  |
| 5               | Left - 7.9<br>Right - 8.4   | Left - 3.6<br>Right - 3.5                         | Posterior<br>126.2°                   | Left not visible<br>Right visible         | 1.0  |
| 6               | Left - 10.1<br>Right - 10.3 | Left - 5.6<br>Right - 4.4                         | Posterior<br>137.3°                   | Left visible<br>Right not visible         | 1.5  |

2.4 mm. The vertical height of the ligaments ranged from 7.1 mm to 12.4 mm with a mean height of 9.8 mm. A detailed summary of the characteristics of individual transverse ligaments examined is provided in Table 3.

In horizontal section, the transverse ligament is seen as a broad, clearly distinguishable band arcing around the posterior aspect of the odontoid process. Concave anteriorly, it consists of parallel fibers running between tubercles situated on either side of the medial aspect of the lateral masses of the atlas [Figure 8].

Measured in the midline, the specimens examined had a mean anterior to posterior thickness of 3.44 mm. As the ligaments progressed toward their insertion onto the atlantal tubercles, a broadening of the ligament was observed in all specimens, which served to increase the surface area of attachment of each end of the ligament. Immediately proximal to the attachments, the mean thickness of the transverse ligaments examined increased to 4.7 mm. This was achieved through a flattening of the posterior margin of the ligament such that

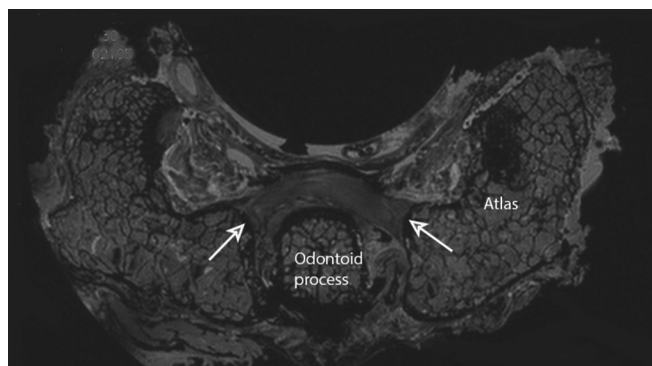


Figure 8: The transverse ligament in axial view acquired using imaging at 4.6T. The atlantal tubercles for attachment of the transverse ligament are indicated by white arrows

the curve formed by this margin followed a greater radius than the anterior margin. The mean length of the posterior margin of the transverse ligament, measured tubercle to tubercle, was 26.7 mm. The anterior margins examined in this series had a mean length of 21.8 mm. A summary of the characteristics of individual transverse ligaments is provided in Table 3.

### Dissection of the imaged specimens

#### Alar ligaments

The alar ligaments of the six specimens imaged each consisted of a single band of dense connective tissue extending from either the lateral or posterolateral aspect of the odontoid process to the occiput. The orientation of these bands appeared primarily horizontal when examined in the coronal plane. One specimen exhibited a single ligament oriented in a cephalad-directed manner and one specimen had a single ligament oriented in a caudal direction as they passed toward their occipital attachment. No atlantal portion of the alar ligaments was observed in any specimen.

When examined from above, all alar ligaments were oriented posteriorly. The actual angle of orientation differed between and within specimens such that the angle with respect to the sagittal plane displayed considerable variation.

Medially, attachment to the odontoid process occurred over a broad area. The alar ligaments of two specimens were observed to extend as far cephalad as the tip of the odontoid process, while the superior margin of other alar ligaments was measured up to 5 mm below this tip. The mean distance of attachment below the tip of the odontoid process was 2.3 mm.

The length and height of each alar ligament were measured *in situ* before blunt dissection of these structures. The mean

Table 3: Measurements and observations obtained from 4.6-tesla magnetic resonance imaging examination of the transverse ligaments in sagittal and axial views

| Specimen number | Sagittal view                           |                      | Horizontal view                         |                                |                                 |  |
|-----------------|---|----------------------|---|--------------------------------|---------------------------------|--|
|                 | Midline antero-posterior thickness (mm) | Vertical height (mm) | Midline antero-posterior thickness (mm) | Length of anterior margin (mm) | Length of posterior margin (mm) | Antero-posterior thickness by atlantal tubercle (mm) |
| 1               | 1.2                                     | 7.1                  | 2.1                                     | 24.6                           | 31.9                            | Left - 5.2<br>Right - 5.7                            |
| 2               | 3.0                                     | 12.4                 | 5.2                                     | 16.9                           | 25.9                            | Left - 4.9<br>Right - 5.7                            |
| 3               | 2.6                                     | 9.6                  | 2.7                                     | 23.5                           | 26.8                            | Left - 4.8<br>Right - 4.6                            |
| 4               | 3.2                                     | 10.2                 | 3.7                                     | 20.2                           | 24.2                            | Left - 4.5<br>Right - 4.7                            |
| 5               | 2.0                                     | 9.5                  | 4.2                                     | 21.1                           | 23.8                            | Left - 3.4<br>Right - 3.7                            |
| 6               | 2.6                                     | 9.8                  | 2.8                                     | 24.4                           | 27.7                            | Left - 5.2<br>Right - 4.7                            |

length of the ligaments was 11.1 mm (range 8 mm–13 mm). Height of the ligament was ascertained immediately adjacent to the odontoid process. The mean height at this point was calculated as 7 mm (range 4 mm–10 mm).

Four of the six specimens exhibited transverse elements of their alar ligaments composed of a group of fibers traversing between the occipital condyles without attachment to the odontoid process. When present, the thickness of these transverse elements varied from approximately 1 mm to several millimeters. All specimens exhibited the majority of the fibers of the alar ligaments attaching to the odontoid process.

Observations on the contribution of the alar ligaments to the area immediately surrounding the atlantooccipital joint varied. In three specimens, some fibers from the alar ligaments appeared to communicate with the medial aspect of both the left and right atlantooccipital joints. In one specimen, this observation was reported on the right side only. In the remaining two specimens, the alar ligaments were described as attaching adjacent to the atlantooccipital joints but could not be observed to communicate or interdigitate directly with the joint capsule itself.

The characteristics of individual alar ligaments noted during dissection are provided in Table 4.

### Cruciform and transverse ligaments

Both ascending and descending cruciform ligaments were observed in each of the six specimens examined. The

ascending cruciform ligaments arose from the superior surface of the transverse ligament, passing in a cephalad direction and inserting onto the clivus. Ascending cruciform ligament length ranged from 12 mm to 17 mm (mean length 14 mm, standard deviation 2 mm). The triangular descending cruciform ligaments extended from the inferior aspects of the transverse ligament, attaching to the posterior aspect of the body of the axis. Descending cruciform ligament length ranged from 6 mm to 11 mm (mean length 9.2 mm, standard deviation 1.9 mm).

The transverse ligament was present in all six specimens examined. Elliptical in shape and attaching to the tubercles on the medial aspects of the atlantal ring adjacent to the lateral atlantoaxial joints, measurements of transverse ligament length ranged from 16 mm to 28 mm (mean length 21 mm, standard deviation 4.1 mm). The midline height, superior to inferior, measured from the posterior aspect of the ligament ranged from 9 mm to 15 mm (mean height 11.7 mm, standard deviation 2.3 mm).

## DISCUSSION

The imaging results may be considered in terms of their consistency with the macrostructure of the ligaments observed during fine dissection.

### Alar ligaments

Each alar ligament described from MRI analysis and upon confirmatory dissection consisted of a single defined band of

**Table 4: Observations of the alar ligaments from dissection of the previously imaged specimens**

| Feature                                     | Specimen number                |  |   |   |  |  |
|---|--------------------------------|--|---|---|--|--|
|   | 1                              | 2  | 3   | 4   | 5  | 6  |
| Occipital portion                           | Present                        | Present  | Present   | Present   | Present  | Present                                  |
| Length (mm)                                 |                                |  |   |   |  |  |
| Left  | 12                             | 10   | 13  | 12  | 11   | 13                                       |
| Right                                       | 9                              | 10   | 11  | 12  | 8  | 12                                       |
| Height medial (mm)                          |                                |  |   |   |  |  |
| Left  | 4                              | 6  | 7   | 6   | 7  | 9  |
| Right                                       | 6                              | 8.5  | 7   | 7   | 6  | 10                                       |
| Atlantal portion                            | Absent                         | Absent   | Absent  | Absent  | Absent   | Absent                                   |
| Ligament orientation                        | Horizontal                     | Left caud-ceph<br>Right horizontal             | Horizontal                                      | Horizontal                                      | Left horizontal<br>Right ceph-caud             | Horizontal                               |
| Aspect of attachment on odontoid            | Lateral and postero-lateral    | Lateral and postero-lateral                    | Primarily postero-lateral                       | Not observed                                    | Not observed                                   | Not observed                             |
| Attachment distance (mm) below odontoid tip | 0                              | 5  | 3.5   | 3   | 0  | Not reported                             |
| Transverse band                             | Present approximate 1 mm thick | Not present                                    | Present approximate 1 mm thick                  | Substantial band several mm in thickness        | Not present                                    | Present and substantial                  |
| Attachment to atlantooccipital joints       | Present left and right         | Attachments adjacent but not visibly into O-C1 | Attachment of fibers into left and right joints | Attachment of fibers into left and right joints | Attachments adjacent but not visibly into O-C1 | Visible attachment into right O-C1 joint |

Caud-ceph - Caudad to cephalad; Ceph-caud - Cephalad to caudad

tissue extending from the odontoid process to the occiput. No atlantal or anterior portions of the ligament as have been previously described<sup>[17,18]</sup> were noted on either method of assessment in any specimen.

Both methods of analysis detailed the medial attachment of the ligaments to the lateral and posterolateral aspect of the odontoid process in all specimens. One specimen on imaging and two specimens on dissection were described as having superior attachments to the tip of the odontoid process. Specimen 1 was observed and measured as attaching to the odontoid tip in both analyses while specimen 5 was described as attaching to the tip on dissection but measured as attaching 0.7 mm below the tip on imaging. This demonstrated consistency in identifying similar characteristics between specimens examined by both dissection and high-resolution imaging. The difference in observation of 0.7 mm in regard to specimen 5 is accounted for by not only the small magnitude of the distance measured but also the fact that the measurements created using MRI are taken at cross-sections of the specimen, whereas the specimen prior to dissection is viewed complete. In addition, being processed digital data, images are viewed at considerable magnification making measurement of intervals possible which may be too small to assess under conditions of gross observation of the specimen.

When viewed in the frontal plane, the assessed orientation of the alar ligaments was primarily horizontal in 10 of the 12 ligaments using both imaging and dissection methods. Due to the concave nature of the specimens, it was not possible to precisely measure the angles created by the ligaments using a protractor; hence, only the subjective observation is reported. The observations again are consistent with the measurements taken of the imaged specimens, with 10 of the 12 alar ligaments measured reported to be within 10° of horizontal. In horizontal plane examination, all alar ligaments were reported to be oriented obliquely posteriorly both on imaging and gross examinations, with included angles ranging from 119° to 173° on MRI assessment.

The assessment of alar ligament length was less when measured in the images of the specimens (mean length 9.5 mm, range 6.9–11.1 mm) than in the specimens during dissection (mean length 11.1 mm, range 8–13 mm). This may be due to the inability to use a straight ruler within a concave bony arrangement, potentially introducing measurement error into this estimate. Superior-inferior height of the ligament adjacent to the odontoid process was more easily measured in the specimens during dissection, and this is reflected in the consistency of measurements taken using both assessment methods. The mean ligament

height measured using coronal plane section images was 7.0 mm (range 4.6–9.4 mm), and the mean height measured during dissection was 7 mm (range 4–10 mm).

Each of the specimens examined had their medial attachment to the odontoid process. However, there was also evidence of the presence of traversing fibers which extended between occipital attachments without an odontoid process attachment. Five specimens were identified as having this band of traversing fibers present on MRI examination. The existence of four of these bands could be confirmed upon subsequent dissection. Specimen 2 was correctly identified as not containing a traversing band on both examinations. Specimen 5 was reported as having a traversing band on MRI examination which could not be confirmed on dissection. The reason for this inconsistency is uncertain given that the observations from the other five specimens are consistent not only in reporting the presence of this element of the alar ligaments but also in their descriptions of the magnitude of each of the traversing bands themselves.

The contribution of fibers from alar ligaments into the medial aspects of the atlantooccipital joints was confirmed using both methods of examination. Using MRI, six of 12 assessed alar ligaments were noted to contribute fibers to the medial aspect of the joints when viewed in coronal section, and all 12 alar ligaments appeared to provide fibers to the medial aspect of the joints when viewed in axial section. Seven alar ligaments were clearly identified as contributing to the atlantooccipital joints on dissection of the specimens while the remaining five were all reported as attaching immediately adjacent to the joint.

### Cruciform and transverse ligaments

Compared to other ligamentous structures assessed using MRI, the cruciform ligaments were poorly defined. The ascending cruciform ligament was observed and measured in four of the six imaged specimens. The descending cruciform ligament was not clearly differentiated from surrounding tissue in any specimen. On dissection, both ligaments were noted to be present in all six specimens. The cruciform ligaments are best viewed on MRI in sagittal section where they can be recognized in cross-section. The descending cruciform ligaments are both shorter and thinner than their ascending counterparts making differentiation of the descending cruciform ligaments from the tectorial membrane and the dura mater more difficult.

Description of the structure of the transverse ligaments was consistent between the high-resolution images and the dissection reports. On both forms of reporting, the



transverse ligament was noted to be an anteriorly concave structure located against the odontoid process. Attachment to the medial tubercles of the atlantal ring was noted in both assessments. The assessment of the dimensions of the structure was not consistent between methods of examination. Measurements of length of the ligament on dissection were consistently less than lengths measured using MRI. Again, this is most likely related to the transverse measurement of a curved structure within a concave bony arrangement. Measurements of superior-inferior height of the transverse ligament on dissection were more similar to measurements obtained from the images, with measurements from the dissection being slightly larger for each specimen.

## CONCLUSION

Overall, the images acquired using 4.6T MRI provide accurate detail of the radiological appearance of the craniovertebral ligaments. The images were representative of these structures when dissected, and the morphology described radiologically is consistent with and confirms findings obtained by gross dissection.

## Financial support and sponsorship

Nil.

## Conflicts of interest

There are no conflicts of interest.

## REFERENCES

1. Kaale BR, Krakenes J, Albrektsen G, Wester K. Active range of motion as an indicator for ligament and membrane lesions in the upper cervical spine after a whiplash trauma. *J Neurotrauma* 2007;24:713-21.
2. Klein GN, Mannion AF, Panjabi MM, Dvorak J. Trapped in the neutral zone: Another symptom of whiplash-associated disorder. *Eur Spine J* 2001;10:141-8.
3. Puttlitz CM, Goel VK, Clark CR, Traynelis VC, Scifert JL, Grosland NM. Biomechanical rationale for the pathology of rheumatoid arthritis in the craniovertebral junction. *Spine* 2000;25:1607-16.
4. Vetti N, Alsing R, Kråkenes J, Rorvik J, Gilhus NE, Brun JG, *et al.* MRI of the transverse and alar ligaments in rheumatoid arthritis: Feasibility and relations to atlantoaxial subluxation and disease activity. *Neuroradiology* 2010;52:215-23.
5. Yochum TR, Rowe LJ. Arthritides of the upper cervical complex. In: Glasgow EF, Twomey LT, Scull ER, Kleynhans AM, Ideczak RM, editors. *Aspects of Manipulative Therapy*. Edinburgh: Churchill Livingstone; 1985.
6. Baumert B, Wortler K, Steffinger D, Schmidt GP, Reiser M, Baur-Melnyk A. Assessment of the internal craniocervical ligaments with a new magnetic resonance imaging sequence: Three-dimensional turbo spin echo with variable flip-angle distribution (SPACE). *Magn Reson Imaging* 2009;27:954-60.
7. Westbrook C, Kaut Roth C, Talbot J. *MRI in Practice*. Chichester: Wiley-Blackwell; 2011.
8. Willauschus WG, Kladny B, Beyer WF, Gluckert K, Arnold H, Scheithauer R. Lesions of the alar ligaments: *In vivo* and *in vitro* studies with magnetic resonance imaging. *Spine* 1995;20:2493-8.
9. Krakenes J, Kaale BR, Rorvik J, Gilhus NE. MRI assessment of normal ligamentous structures in the craniovertebral junction. *Neuroradiology* 2001;43:1089-97.
10. Kim HJ, Jun BY, Kim WH, Cho YK, Lim MK, Suh CH. MR imaging of the alar ligament: Morphologic changes during axial rotation of the head in asymptomatic young adults. *Skeletal Radiol* 2002;31:637-42.
11. Pfirrmann CW, Binkert CA, Zanetti M, Boos N, Hodler J. MR morphology of alar ligaments and occipito-atlantoaxial joints: Study in 50 asymptomatic subjects. *Radiology* 2001;218:133-7.
12. Dickman CA, Mamourian A, Sonntag VK, Drayer BP. Magnetic resonance imaging of the transverse atlantal ligament for the evaluation of atlantoaxial instability. *J Neurosurg* 1991;75:221-7.
13. Krakenes J, Kaale BR, Nordli H, Moen G, Rorvik J, Gilhus NE. MR analysis of the transverse ligament in the late stage of whiplash injury. *Acta Radiol* 2003;44:637-44.
14. Dvorak J, Schneider E, Saldinger P, Rahn B. Biomechanics of the craniocervical region: The alar and transverse ligaments. *J Orthop Res* 1988;6:452-61.
15. Magnitsky S, Watson DJ, Walton RM, Pickup S, Bulte JW, Wolfe JH, *et al.* *In vivo* and *ex vivo* MRI detection of localized and disseminated neural stem cell grafts in the mouse brain. *Neuroimage* 2005;26:744-54.
16. Osmotherly PG, Rivett DA, Mercer SR. Revisiting the clinical anatomy of the alar ligaments. *Eur Spine J* 2013;22:60-4.
17. Dvorak J, Panjabi MM. Functional anatomy of the alar ligaments. *Spine (Phila Pa 1976)* 1987;12:183-9.
18. White AA, Panjabi MM. *Clinical Biomechanics of the Spine*. Philadelphia: J.B. Lippincott Company; 1990.